arXiv:1211.1290v1 [cond-mat.other] 6 Nov 2012

Condensation of exciton-polaritons through evaporative cooling

A. Askitopoulos[1], H. Ohadi[1], Z. Hatzopoulos[2,4], P.G. Savvidis[2,3], A.V. Kavokin[1,5], and P.G. Lagoudakis *[1]

[1]School of Physics and Astronomy, University of Southampton, Southampton, SO17 1BJ, United Kingdom
[2]Foundation for Research and Technology - Hellas, Institute of Electronic Structure and Laser, PO Box 1527, 71110 Heraklion, Crete, Greece
[3]Department of Materials Science and Technology, University of Crete, PO Box 2208, 71003 Heraklion, Crete, Greece
[4]Department of Physics, University of Crete, PO Box 2208, 71003 Heraklion, Crete, Greece
[5]Spin Optics Laboratory, St-Petersburg State University, 1, Ulianovskaya, St-Peterbsurg, 198504, Russia

Evaporative cooling has led to the coldest temperatures ever observed in the universe: sub-microkelvin temperatures generated in atom traps. It turned out to be the key technique to achieve Bose-Einstein condensation, a long-sought goal in atomic physics [1–3]. Evaporation describes the process of energetic particles leaving a system with a finite binding energy [5,6]. This process results in cooling: since the evaporating particles carry away more than their share of thermal energy, the temperature of the system decreases. Here we demonstrate experimentally the condensation of exciton-polaritons through evaporative cooling. A cold fraction of exciton-polaritons condenses in an optically induced two-dimensional trap inside the crystal, decoupled from the decoherence inducing excitonic reservoir [6]. We detect a characteristic Bogolyubov dispersion of the condensate with a sound velocity proportional to the square root of the number of trapped quasiparticles and extract the polariton-polariton interaction strength. In a reference experiment, where the evaporative cooling mechanism is switched off by changing the excitation intensity profile, polariton condensation takes place for excitation densities one order of magnitude higher and the resulting condensate is subject to

---

*pavlos.lagoudakis@soton.ac.uk

a much stronger dephasing. These observations pave the way to the realisation of polariton logic devices including optically controlled transistors and ultrafast switches as well as the study of bosonic superfluid effects in semiconductor microcavities.

Strong coupling of cavity photons and quantum-well excitons gives rise to mixed light-matter bosonic quasiparticles called exciton-polaritons or polaritons[7]. Due to their photonic component, polaritons are several orders of magnitude lighter than atoms, which makes their Bose-Einstein condensation (BEC) attainable at higher temperatures. In an ideal infinite two-dimensional cavity the polariton gas is expected to undergo the Berezinsky-Kosterlitz-Thouless (BKT) phase transition[8], while in realistic structures, polaritons can condense in traps induced by random disorder[9], mechanical[10,11] or optical[12–14] potentials. Polariton condensation has been also observed in the structures of lower dimensionality[15–17]. The manifestations of polariton condensation include polariton lasing[18], long-range spatial coherence[9] and stochastic vector polarisation[19]. Being weakly-interacting bosons, polaritons are expected to show the characteristic Bogolyubov linear dispersion in the condensed phase[20]. Experimental efforts to observe this kind of dispersion[8,22] are met with difficulties. Depletion of the condensate due to its interaction with the background excitons and uncondensed polaritons in the reservoir leads to the broadening of photoluminescence, which makes it hard to distinguish between linear and parabolic dispersions in the vicinity of the ground state.

Here we have designed and implemented a ring-shaped optical trap, which allows for efficient evaporative cooling of polaritons[23] and formation of a condensate spatially separated from the excitonic reservoir. This is achieved by nonresonant excitation of a planar microcavity sample by a laser beam in the shape of a ring. The diameter of the ring is 20 μm, which is of the order of the polariton mean free path in planar microcavities and much larger than the exciton diffusion length in the quantum wells that we study[2].

The nonresonant excitation creates a hot electron-hole plasma, which then forms excitons. Hot excitons cool down by exciton-phonon scatterings. When they enter the light cone they couple strongly to the cavity mode and populate the lower polariton branch on the ring. Excitons diffuse around the excitation area but due to their large effective mass they are unable to reach the center of the ring. The repulsion of polaritons from the ring-shape exciton reservoir can be described by a mean-field ring-like trapping potential, which is approximately 1 meV deep in the center at the pumping power corresponding to the condensation threshold. Uncondensed polaritons start from the blueshifted states on the ring and ballistically expand[25] either towards the center or outside. Those which fly to the center eventually collide with each other (see Fig 1). The energy of the ensemble of polaritons is conserved by these scattering events, so that the kinetic energies of approx-

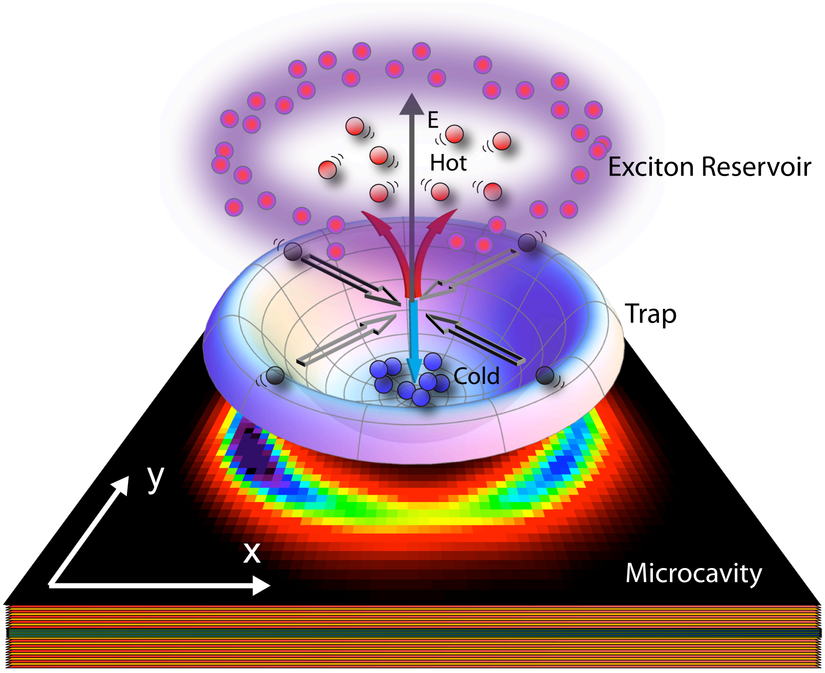

Figure 1: **Evaporative cooling in a ring-shaped polariton trap.** Polariton trap over real space excitation spot, displaying the parametric scattering assisted evaporative cooling mechanism. High energy and momentum polaritons scattered to high energy states leave the trap, while polaritons scattered to low energy and momentum remain confined.

imately half of the polaritons are reduced, while the other half have their kinetic energies increased[26]. As a result, a cold and a hot fraction of the polariton gas are being formed. The cold fraction is no more capable to escape from the trap due to the lack of kinetic energy, while polaritons from the hot fraction can easily fly away across the barriers. Further scatterings of the trapped polaritons lead to the increase of the kinetic energy of some of them so that they become able to leave the trap. Eventually, the polariton gas in the trap cools down below the critical temperature for BEC in close analogy to atomic gases in dipole and magnetic traps[4] (see Supplementary Information, S2). The condensate forms at the center of the trap and then quickly builds up due to stimulated scattering of the trapped polaritons.

Fig. 2a-c shows the real-space images of the photoluminescence (PL) below threshold, at threshold and above threshold pumping powers, respectively (see also supplementary movie). Above threshold a Gaussian shaped condensate, with full width at half maximum (FWHM) of $5.46\,\mu$m and standard deviation $\sigma_x = 2.32\,\mu$m, is formed inside the ring. The fringes observed by Michelson interferometry (Supplementary Information, S4) in this regime confirm the coherence of the condensate (see the inset in Fig. 2c).

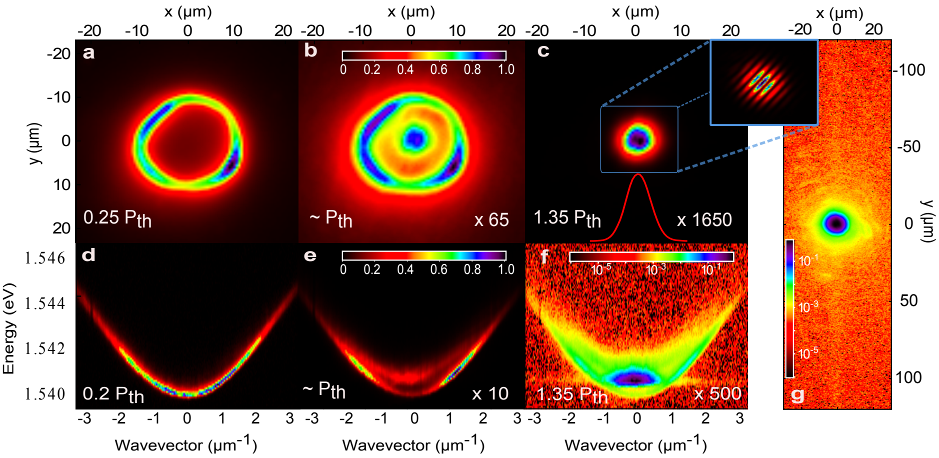

Figure 2: **Single-mode exciton-polariton condensate in a ring-shaped trap.** Emission images in real space below (**a**), at (**b**) and above threshold (**c**). The inset in **c** shows the interference fringes of the condensate. Red line is the condensate profile along the x axis. Polariton condensation is clearly visible in the center of the ring and is separate from the excitation spot outlined by the emission in **a**. **d, e, f** Dispersion images below (**d**), at (**e**) and above (**f**) threshold. **g**, Same as (**c**) but with a logarithmic colourscale showing that the condensate propagation beyond the trap is minimal.

Fig. 2d-f shows the dispersion of polaritons at different pumping powers. Below threshold we observe a parabolic lower polariton branch. As soon as the polariton density in the centre of the ring is increased close to the threshold, we observe a blueshifted dispersion from polaritons in the trap, coexisting with the parabolic dispersion of untrapped polaritons as it will become evident further on from spatially resolved dispersion imaging. The two lobes of the outer dispersion correspond to hot polaritons escaping from the centre of the ring. By further increasing the excitation power a condensate appears in the ground state of the blueshifted dispersion with zero in-plane momentum and standard deviation $\sigma_{k_x} = 0.22\,\mu\text{m}^{-1}$, shown in logarithmic scale in Fig. 2f. The macroscopically occupied ground state is Heisenberg limited ($\sigma_x \sigma_{k_x} = 0.51$), which confirms that phase fluctuations in the condensate are strongly reduced.

The spatially-resolved dispersion images in Fig. 3a and Fig. 3b show that untrapped polaritons situated far away from the center of the ring have high energies and large wavevectors, while those in the center of the trap populate mostly the lower states even at pump powers much below threshold. The dispersion of the polaritons on the rim of the ring does not change greatly with increasing power, while the dispersion images at the center of the trap show condensation at $k = 0$ state above threshold. Fig. 3c shows the energy

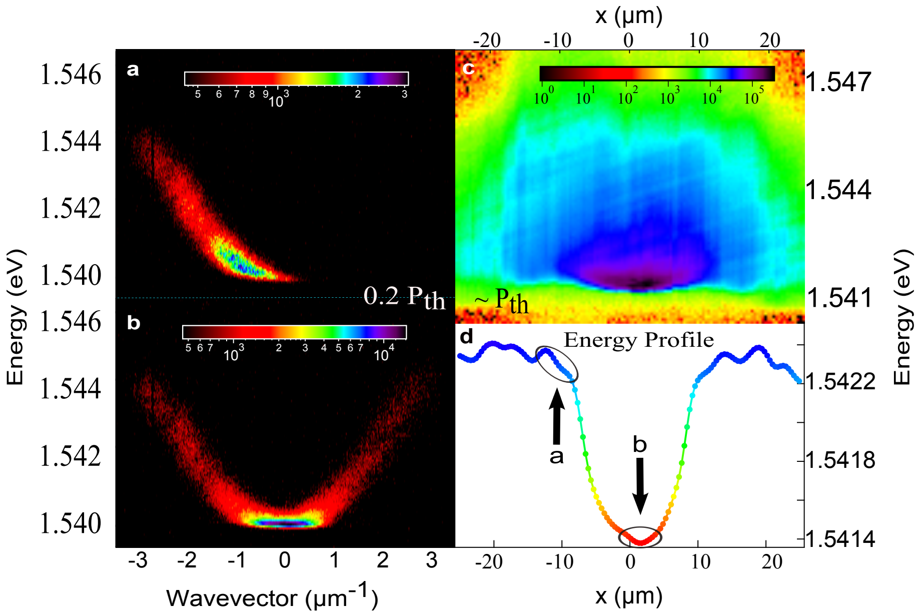

Figure 3: **Trapping potential and spatially-resolved dispersions. a, b,** Dispersion images below threshold ($P = 0.2P_{th}$) from a $5\,\mu$m diameter spatially filtered region from the rim of the ring (**a**) and the center (**b**). Energy profile of the central slice of the ring at threshold (**c**) and the extracted maxima of intensity along the x axis for the visualization of the trap profile(**d**). Points a and b correspond to **a** and **b** respectively.

spectrum of a slice through the center of the ring excitation at the onset of condensation. Fig. 3d shows the profile of the trap potential extracted from the intensity maximum along each point on the x axis in Fig. 3c. The trap depth at the power just below the threshold is $\sim 1\,$meV. The two circles annotate the points where the spatially filtered dispersions were acquired.

The full spatial separation of the condensate from the pump induced excitonic reservoir has important implications on the spectral and dynamic properties of polaritons[6] even below threshold. Due to the efficient stimulated scattering process we observe significantly lower power densities for condensation. In a reference experiment we have excited the same sample (at the same detuning and temperature) with a normal Gaussian beam with a spot size of $\sim 5\,\mu$m. Fig. 4a shows the normalized PL intensity of $k = 0$ for different excitation powers. The threshold power density is an order of magnitude higher in the case of Gaussian excitation. Contrary to previous works, we observe condensation spatially delocalised from the excitation area and prior to the build up of coherence in the excitation area.

A clear advantage of separation of the condensate from the feeding reservoir is in the strong reduction of the depletion processes caused by

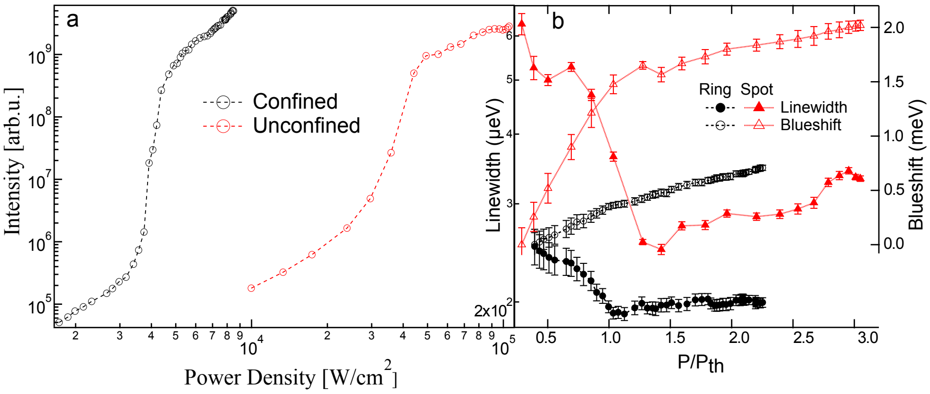

Figure 4: **Normalized intensity, linewidth and blueshif.** **a**, Normalized intensity with increasing power density for polaritons in the center (open black dots) of the ring excitation, and for a Gaussian excitation (open red circles) measured at k=$0 \pm 0.05\,\mu$m^{-1} of the spatially filtered dispersion. **b**, Linewidth (in log scale) and blueshift vs. excitation power for polaritons at the center of the ring (black circles, open black circles respectively) and a Gaussian excitation (red triangles, open red triangles respectively). Lines are guides for the eyes.

condensate-reservoir interactions[17]. Fig. 4b shows the linewidth and blueshift of the condensate for the ring and Gaussian excitation cases. Clearly, in the case of ring-excitation condensate, due to the absence of decoherence mechanisms by the background reservoir, the linewidth is narrower and it increases much slower than in the Gaussian excitation, reflecting the reduced interactions in the condensate and showing that dephasing is substantially suppressed[28]. The blueshift of the condensate increases linearly with the pumping intensity, in the case of ring-like excitation, showing the linear increase of the mean number of condensed polaritons. In the case of Gaussian excitation, the blue shift is strongly affected by the reservoir: it is twice as large as in the ring-excitation case and slowly saturates above threshold, indicating that exciton saturation has been reached[29].

The Bogolyubov dispersion is a theoretically expected feature of polariton condensates and superfluids[8]. The repulsive interaction of polaritons renormalizes the parabolic energy spectrum at low momenta given by $E_k^0 = \hbar^2 k^2/2m$, m being the effective polariton mass, into a near linear (sound-like) dispersion. The Bogolyubov excitation energy is given by

$$E_k = \sqrt{2nU_0E_k^0 + (E_k^0)^2} = nU_0\sqrt{(k\xi)^2[(k\xi)^2 + 2]},$$

where n is the occupation number of the condensate, U_0 is polariton-polariton interaction potential, and $\xi = \hbar/(\sqrt{2}ms)$ is the healing length. For small k, the excitation energy is $E_k \simeq s\hbar k$, where $s = \sqrt{nU_0/m}$ is the speed of

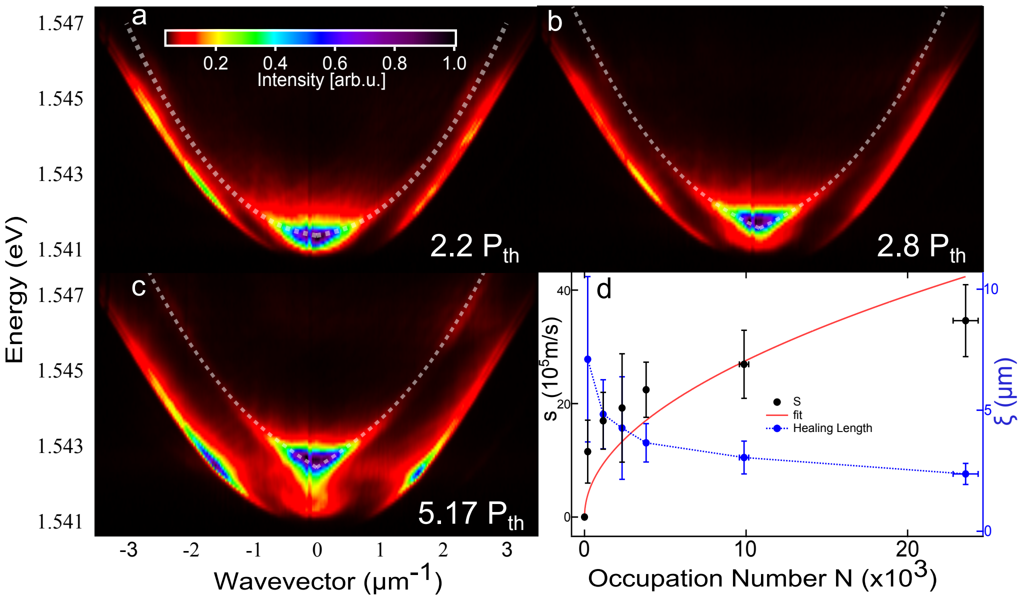

Figure 5: **Bogolyubov dispersions and the speed of sound.** The dispersion images of the confined condensate at $2.2P_{th}$ (**a**), $P = 2.8P_{th}$ (**b**) and $P = 5.17P_{th}$ (**c**) are shown. The dispersion is clearly linear for small wave vectors, in stark contrast to the quadratic uncondensed polariton dispersion from the ring. White lines are fits of theoretical Bogolyubov dispersion **d**, Speed of sound and the healing length in the condensate extracted from the slope of the linear dispersion.

sound.

Previous reports of the Bogolyubov dispersion in polariton condensates[22] have also revealed a diffusive Goldstone dispersion which originates from the condensate diffusion in an inhomogeneous excitation area. Creating the condensate by evaporative cooling in the centre of the excitation ring allows for the observation of a Bogolyubov dispersion in the absence of condensate diffusion and scattering with the excitonic reservoir. The appearance of a linear dispersion can be noticed already at the threshold power as Fig. 2e shows. By further increasing the excitation density up to 25 times above threshold a strong modification of the dispersion is observed (see Fig. 5a-c). The slope is proportional to the square root of the condensate density, which is linearly dependent on the pumping power above threshold (see Fig. 4a). Fig. 5d shows the speed of sound extracted from the linear dispersion versus occupation number revealing a good agreement with previously reported values[8] (see Supplementary Information, S3) taking $U_0 = 0.043\,\mu$eV. The healing length becomes $\sim 7\,\mu$m at threshold, which is comparable to half the size of the trap ($\sim$ FWHM$= 15\,\mu$m). By increasing the excitation power and the occupation number of the condensate, the healing length ξ is reduced reflecting the filling of the trap by the condensate. The speed of sound ranges between 5×10^5 m/s and 35×10^5 m/s in good agreement with the theoretical prediction[7].

In conclusion, we have demonstrated the evaporative cooling of a dilute polariton bosonic gas in a two-dimensional trap created by ring-shaped nonresonant excitation. This configuration allows for the formation of a polariton condensate spatially separated from the excitation area minimizing dephasing and depletion processes. We have observed renormalisation of the Bogolyubov excitation spectrum on the excitation density and verified the square root dependence of the speed of sound on the occupation number of the condensate.

Methods

The sample is a high Q GaAs/AlGaAs microcavity containing four separate triplets of 10 nm GaAs quantum wells[30]. It was held at ~ 6.5 K in a cold-finger cryostat and excited nonresonantly at the first reflection minimum above the cavity stop band with a single-mode continuous wave laser and a pulsed laser for the higher powers presented for the Bogolyubov dispersions. The excitation beam profile was shaped into a ring in real space with the use of two axicons and was projected onto the microcavity through an objective lens ($\mathrm{NA} = 0.4$) creating a polariton ring with a mean diameter of $\sim 19\,\mu$m on the sample (Supplementary Information, S1). The excitation beam intensity was modulated with an accousto-optic modulator at 1% duty cycle with a frequency of 10 kHz to reduce heating of the sample.

Acknowledgements

We acknowledge funding from Marie Curie ITNs Spinoptronics, Clermont IV and EPSRC through Contract No. EP/F026455/1. P.G.S. acknowledges funding from the EU Social Fund and Greek National Resources (EPEAEK II, HRAKLEITOS II).

References

1. Anderson, M. H., Ensher, J. R., Matthews, M. R., Wieman, C. E. & Cornell, E. A. Observation of Bose-Einstein condensation in a dilute atomic vapor. *Science* **269**, 198 –201 (1995). URL http://www.sciencemag.org/content/269/5221/198.abstract.

2. Bradley, C. C., Sackett, C. A., Tollett, J. J. & Hulet, R. G. Evidence of Bose-Einstein condensation in an atomic gas with attractive interactions. *Physical Review Letters* **75**, 1687–1690 (1995). URL http://link.aps.org/doi/10.1103/PhysRevLett.75.1687.

3. Davis, K. B. *et al.* Bose-Einstein condensation in a gas of sodium atoms. *Physical Review Letters* **75**, 3969–3973 (1995). URL http://link.aps.org/abstract/PRL/v75/i22/p3969http://link.aps.org/pdf/PRL/v75/i22/p3969.

4. Luiten, O. J., Reynolds, M. W. & Walraven, J. T. M. Kinetic theory of the evaporative cooling of a trapped gas. *Physical Review A* **53**, 381–389 (1996). URL http://link.aps.org/doi/10.1103/PhysRevA.53.381.

5. Berg-Sørensen, K. Kinetics for evaporative cooling of a trapped gas. *Physical Review A* **55**, 1281–1287 (1997). URL http://link.aps.org/doi/10.1103/PhysRevA.55.1281.

6. Vishnevsky, D. V., Solnyshkov, D. D., Gippius, N. A. & Malpuech, G. Multistability of cavity exciton polaritons affected by the thermally generated exciton reservoir. *Physical Review B* **85**, 155328 (2012). URL http://link.aps.org/doi/10.1103/PhysRevB.85.155328.

7. Kavokin, A. V., Baumberg, J., Malpuech, G. & Laussy, F. P. *Microcavities* (Oxford Univ. Press, Oxford, 2007).

8. Malpuech, G., Rubo, Y. G., Laussy, F. P., Bigenwald, P. & Kavokin, A. V. Polariton laser: thermodynamics and quantum kinetic theory. *Semiconductor Science and Technology* **18**, S395–S404 (2003). URL http://iopscience.iop.org/0268-1242/18/10/314.

9. Kasprzak, J. *et al.* Bose-Einstein condensation of exciton polaritons. *Nature* **443**, 409–14 (2006). URL http://dx.doi.org/10.1038/nature05131.

10. Balili, R., Hartwell, V., Snoke, D., Pfeiffer, L. & West, K. Bose-Einstein condensation of microcavity polaritons in a trap. *Science* **316**, 1007 –1010 (2007). URL http://www.sciencemag.org/content/316/5827/1007.abstract.

11. Balili, R. B., Snoke, D. W., Pfeiffer, L. & West, K. Actively tuned and spatially trapped polaritons. *Applied Physics Letters* **88**, 031110–031110–3 (2006). URL http://apl.aip.org/resource/1/applab/v88/i3/p031110_s1.

12. Wertz, E. *et al.* Spontaneous formation and optical manipulation of extended polariton condensates. *Nature Physics* **6**, 860–864 (2010). URL http://www.nature.com/nphys/journal/v6/n11/full/nphys1750.html.

13. Tosi, G. *et al.* Sculpting oscillators with light within a nonlinear quantum fluid. *Nat Phys* **advance online publication** (2012). URL http://dx.doi.org/10.1038/nphys2182.

14. Gao, T. *et al.* Polariton condensate transistor switch. *Physical Review B* **85**, 235102 (2012). URL http://link.aps.org/doi/10.1103/PhysRevB.85.235102.

15. Maragkou, M. *et al.* Spontaneous nonground state polariton condensation in pillar microcavities. *Physical Review B* **81**, 081307 (2010). URL http://link.aps.org/doi/10.1103/PhysRevB.81.081307.

16. Bajoni, D. *et al.* Polariton laser using single micropillar GaAs-GaAlAs semiconductor cavities. *Physical Review Letters* **100**, 047401 (2008). URL http://link.aps.org/doi/10.1103/PhysRevLett.100.047401.

17. Ferrier, L. *et al.* Interactions in confined polariton condensates. *Physical Review Letters* **106**, 126401 (2011). URL http://link.aps.org/doi/10.1103/PhysRevLett.106.126401.

18. Christopoulos, S. *et al.* Room-temperature polariton lasing in semiconductor microcavities. *Physical Review Letters* **98**, 126405 (2007). URL http://link.aps.org/doi/10.1103/PhysRevLett.98.126405.

19. Ohadi, H. *et al.* Spontaneous symmetry breaking in a polariton and photon laser. *Physical Review Letters* **109**, 016404 (2012). URL http://link.aps.org/doi/10.1103/PhysRevLett.109.016404.

20. Bogoliubov, N. N. On the theory of superfluidity. *urnal of Physics-USSR* **11**, 23 (1947).

21. Utsunomiya, S. *et al.* Observation of Bogoliubov excitations in exciton-polariton condensates. *Nature Physics* **4**, 700–705 (2008). URL http://www.nature.com/nphys/journal/v4/n9/full/nphys1034.html#a3.

22. Aßmann, M. *et al.* From polariton condensates to highly photonic quantum degenerate states of bosonic matter. *Proceedings of the National Academy of Sciences* (2011). URL http://www.pnas.org/content/early/2011/01/13/1009847108.

23. Berman, O. L., Lozovik, Y. E. & Snoke, D. W. Evaporative cooling and condensation of two-dimensional polaritons in an in-plane harmonic potential. *physica status solidi (c)* **3**, 3373–3377 (2006). URL `http://onlinelibrary.wiley.com/doi/10.1002/pssc.200672107/abstract`.

24. Heller, W., Filoramo, A., Roussignol, P. & Bockelmann, U. Direct measurement of exciton diffusion in quantum wells. *Solid-State Electronics* **40**, 725–728 (1996). URL `http://www.sciencedirect.com/science/article/pii/0038110195003517`.

25. Kammann, E. *et al.* Nonlinear optical spin hall effect and long-range spin transport in polariton lasers. *Physical Review Letters* **109**, 036404 (2012). URL `http://link.aps.org/doi/10.1103/PhysRevLett.109.036404`.

26. Savvidis, P. G. *et al.* Angle-Resonant stimulated polariton amplifier. *Physical Review Letters* **84**, 1547–1550 (2000). URL `http://link.aps.org/doi/10.1103/PhysRevLett.84.1547`.

27. Ketterle, W., Druten, N. V., Bederson, B. & Walther, H. Evaporative cooling of trapped atoms. In *Advances In Atomic, Molecular, and Optical Physics*, vol. Volume 37, 181–236 (Academic Press, 1996). URL `http://www.sciencedirect.com/science/article/pii/S1049250X08601019`.

28. Porras, D. & Tejedor, C. Linewidth of a polariton laser. *Physical Review B* **67**, 161310 (2003). URL `http://link.aps.org/doi/10.1103/PhysRevB.67.161310`.

29. Holden, T. M., Kennedy, G. T., Cameron, A. R., Riblet, P. & Miller, A. Exciton saturation in room temperature GaAs/AlGaAs multiple quantum wells. *Applied Physics Letters* **71**, 936–938 (1997). URL `http://apl.aip.org/resource/1/applab/v71/i7/p936_s1`.

30. Tsotsis, P. *et al.* Lasing threshold doubling at the crossover from strong to weak coupling regime in GaAs microcavity. *New Journal of Physics* **14**, 023060 (2012). URL `http://iopscience.iop.org/1367-2630/14/2/023060`.

Supplementary Information

S1 Experimental Setup

Using two axicons (conical lenses) (see Fig. **S1**), a collimated ring-shaped beam from a collimated Gaussian beam is generated[1]. The ring diameter can be adjusted by changing the distance between the two axicons. We then use a long distance lens and an objective to project and focus the rim of the ring-shaped beam onto the sample. The same objective is then used for the collection of the emitted light. Real space and dispersion images are acquired with a monochromator equipped with a water cooled charged couple device (CCD).

The excitation laser used in Fig. 2, 3, 4 was a frequency stabilized single-mode Ti:Sapphire laser. The Bogolyubov dispersions were acquired by a pulsed laser since in the pulsed mode the condensate does not suffer from the diffusion of the pump induced excitons into the centre of the trap[2,3]. The laser was a 150 femtosecond pulsed laser with a repetition rate of 80 kHz.

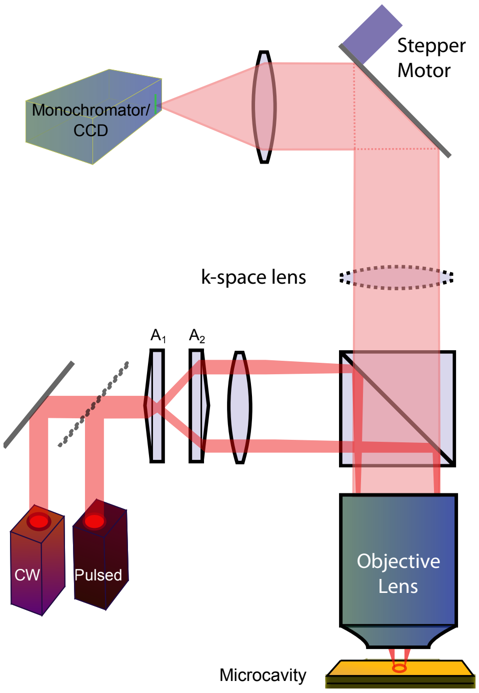

Figure **S1**: Hollow beam generation with axicons used for the polariton trap and the experimental setup used for the acquisition of images.

S2 Evaporative cooling mechanism

In the evaporative cooling technique for cold atoms[4,5] the trap potential is lowered and raised repeatedly. The hot particles escape the trap when the trap depth is shallow. By increasing the trap potential again the trapped particles rethermalize and therefore the total free energy of the system is slightly reduced. The thermalization also promotes particles to energies above the trap depth. This process is repeated until the temperature of the ensemble reaches the critical temperature for Bose-Einstein condensation[6]. In our ring-shaped polariton trap, the extraction of hot particles is achieved by means of stimulated polariton-polariton scatterings. A polariton-polariton scattering event results in a higher and lower energy polariton. The hot polariton escapes the trap leaving a cold polariton in the bottom of the trap. The rate of buildup of occupation in the ground state is increased by final-state stimulated scattering, until a critical density for condensation is achieved.

The polaritons in the centre of the trap experience a blueshift in energy as the density increases due to polariton-polariton interaction. The blueshift is linearly proportional to the density of the condensate. For excitation densities of $0.5P_{th}$ the trap depth is 1.33 meV compared to 1 meV at condensation threshold (Fig. **S2**). This blue shift effectively makes the trapping potential of the condensate shallower as the occupation density in the ground state rises, further increasing the efficiency of cooling.

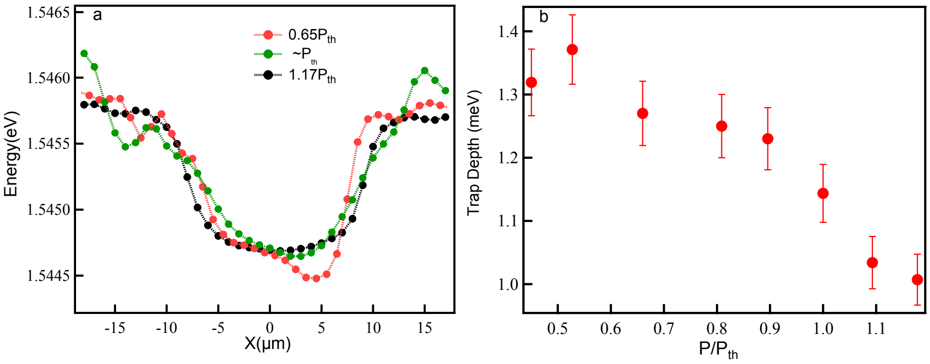

Figure **S2**: **a**, Energy profile of the trap at different excitation densities. **b**, Trap depth evolution with power density.

S3 Polariton-polariton interaction constant and healing length extraction

Extracting the speed of sound $s(n) = \sqrt{nU_0/m}$ from the condensate in the Bogolyubov regime is achieved by measuring the slope of the dispersion for small wavevectors. It is a simple step from there to extract the healing length ($\xi = \hbar/\sqrt{2}ms$) as a function of occupation number. The reduction of the healing length for higher occupation numbers shows clearly that the condensate gradually expands and fills increasingly larger areas of the trap with a uniform density. From $s(n)$ we can extract $\mathrm{U}_0 = g_0^{Pol}/S = 0.043\,\mu\mathrm{eV}$ and $g_0^{Pol} = 22.1 \times 10^{-38}\,\mathrm{Jm}^2$, where $S = 32\,\mu\mathrm{m}^2$ is the condensate area and g_0^{Pol} is the polariton-polariton interaction energy.

Using a numerical estimate for the exciton-exciton interaction[7] we get

$$g_0^{Exc} = 6a_B^2 E_b = 84 \times 10^{-38}\,\mathrm{Jm}^2,$$

where $E_b = 8.7\,\mathrm{meV}$ is the exciton binding energy, $a_B = 12\,\mathrm{nm}$ is the Bohr radius for 10 nm *GaAs* QWs. In order to obtain the polariton-polariton interaction constant g_0^{Pol} one needs to multiply g_0^{Exc} by the 4^{th} power of the exciton Hopfield coefficient X of the polariton state, which is $X^4 = 0.06$ in our case. This yields $g_0^{Pol} = 5.25 \times 10^{-38}\,\mathrm{Jm}^2$. One can see that the interaction constant we obtain is of the same order of magnitude as the theoretical estimate and close to the experimental value of $g_0^{Pol} = 8.9 \times 10^{-38}\,\mathrm{Jm}^2$ for GaAs QWs[8]. The deviation from the theoretical prediction can be ascribed to the spin and wave vector dependence of the interaction constant, which is neglected here.

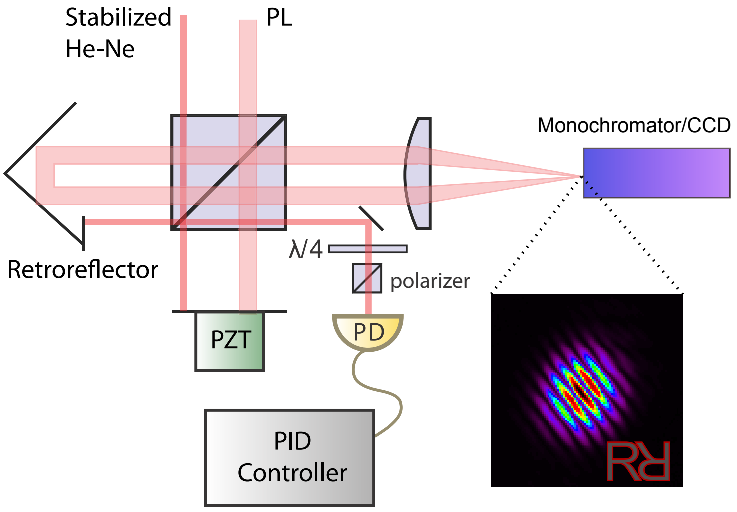

Figure **S3**: Stabilised Michelson interferometer in the retroreflector configuration

S4 Interferometry and Energy Tomography

Interferometric measurements were made using a stabilised Michelson interferometer similar to the one in reference[9], in a mirror-retroreflector config-

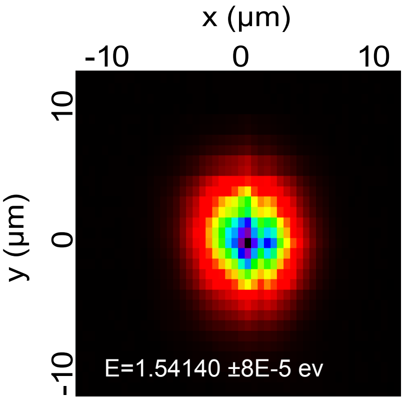

Figure **S4**: Energy tomography of the condensate in real space.

uration with close to zero arm length difference. The arm length difference was actively stabilized by a frequency stabilized He-Ne laser in a PID feedback loop (see Fig. **S3**).

By changing the angle of the last mirror in Fig. **S1** with a computerized translation stage it is possible to scan the entire image from the sample across the 20 μm slit of the spectrometer. Acquiring the spectral images for each position enables us to reconstruct a tomographic real space image at a specific energy (Fig. **S4**) (or more accurately a narrow band of energies equal to the spectral resolution). Energy tomography images reveal that the entire condensate is at the same energy level. This is also verified by interferometric measurements.

References

1. Manek, I., Ovchinnikov, Y. & Grimm, R. Generation of a hollow laser beam for atom trapping using an axicon. *Optics Communications* **147**, 67–70 (1998). URL `http://www.sciencedirect.com/science/article/pii/S0030401897006457`.

2. Heller, W., Filoramo, A., Roussignol, P. & Bockelmann, U. Direct measurement of exciton diffusion in quantum wells. *Solid-State Electronics* **40**, 725–728 (1996). URL `http://www.sciencedirect.com/science/article/pii/0038110195003517`.

3. Nagamune, Y., Watabe, H., Sogawa, F. & Arakawa, Y. One-dimensional exciton diffusion in GaAs quantum wires. *Applied Physics Letters* **67**, 1535–1537 (1995). URL `http://apl.aip.org/resource/1/applab/v67/i11/p1535_s1`.

4. Ketterle, W., Druten, N. V., Bederson, B. & Walther, H. Evaporative cooling of trapped atoms. In *Advances In Atomic, Molecular, and Optical*

Physics, vol. Volume 37, 181–236 (Academic Press, 1996). URL http://www.sciencedirect.com/science/article/pii/S1049250X08601019.

5. Pethick, C. J. & Smith, H. *Bose-Einstein Condensation in Dilute Gases* (Cambridge University Press, 2001).
6. Luiten, O. J., Reynolds, M. W. & Walraven, J. T. M. Kinetic theory of the evaporative cooling of a trapped gas. *Physical Review A* **53**, 381–389 (1996). URL http://link.aps.org/doi/10.1103/PhysRevA.53.381.
7. Tassone, F. & Yamamoto, Y. Exciton-exciton scattering dynamics in a semiconductor microcavity and stimulated scattering into polaritons. *Physical Review B* **59**, 10830–10842 (1999). URL http://link.aps.org/doi/10.1103/PhysRevB.59.10830.
8. Utsunomiya, S. *et al.* Observation of Bogoliubov excitations in exciton-polariton condensates. *Nature Physics* **4**, 700–705 (2008). URL http://www.nature.com/nphys/journal/v4/n9/full/nphys1034.html#a3.
9. Kasprzak, J. *et al.* Bose–Einstein condensation of exciton polaritons. *Nature* **443**, 409–414 (2006). URL http://www.nature.com/nature/journal/v443/n7110/suppinfo/nature05131.html.